

# In situ synchrotron based x-ray fluorescence and scattering measurements during atomic layer deposition: Initial growth of HfO<sub>2</sub> on Si and Ge substrates

K. Devloo-Casier,<sup>1,a)</sup> J. Dendooven,<sup>1</sup> K. F. Ludwig,<sup>2</sup> G. Lekens,<sup>3</sup> J. D'Haen,<sup>3</sup> and C. Detavernier<sup>1</sup>

<sup>1</sup>Department of Solid State Sciences, Ghent University, Krijgslaan 281/S1, B-9000 Ghent, Belgium

<sup>2</sup>Department of Physics, Boston University, 590 Commonwealth Avenue, Boston, Massachusetts 02215, USA

<sup>3</sup>IMEC vzw Division IMOMECE, Wetenschapspark 1, 3590 Diepenbeek, Belgium

(Received 22 April 2011; accepted 18 May 2011; published online 8 June 2011)

The initial growth of HfO<sub>2</sub> was studied by means of synchrotron based *in situ* x-ray fluorescence (XRF) and grazing incidence small angle x-ray scattering (GISAXS). HfO<sub>2</sub> was deposited by atomic layer deposition (ALD) using tetrakis(ethylmethylamino)hafnium and H<sub>2</sub>O on both oxidized and H-terminated Si and Ge surfaces. XRF quantifies the amount of deposited material during each ALD cycle and shows an inhibition period on H-terminated substrates. No inhibition period is observed on oxidized substrates. The evolution of film roughness was monitored using GISAXS. A correlation is found between the inhibition period and the onset of surface roughness. © 2011 American Institute of Physics. [doi:10.1063/1.3598433]

Atomic layer deposition (ALD) is a thin film growth technique which enables thickness control at the atomic level and conformal deposition on high aspect ratio structures.<sup>1,2</sup> These features make the technique ideally suited for micro-electronics applications, mainly for the deposition of high- $\kappa$  gate dielectrics.

ALD processes are characterized by a layer-by-layer type growth, i.e., the thickness increases proportionally to the amount of ALD cycles. This linear regime is, however, only reached after a couple of ALD cycles. During the first cycles, the film growth is determined by chemisorption of precursor molecules on the substrate and, therefore, pretreatment of the substrate surface is critical. It is important to obtain an in depth understanding of the initial nucleation phase as it has a large influence on the characteristics of the deposited film. For high- $\kappa$  dielectrics one looks for a fast nucleation with a subsequent linear growth, because this results in a closed layer after a few ALD cycles, enabling the deposition of gate structures with a low equivalent oxide thickness.<sup>3</sup>

In this letter, we propose the use of synchrotron radiation to study the initial growth phase of ALD processes in real time. Probing the sample with x-rays enables to perform x-ray fluorescence (XRF) and grazing incidence small angle x-ray scattering (GISAXS) measurements. XRF allows to monitor the atomic composition of the film and thus the amount of material deposited during each ALD cycle.<sup>4-6</sup> GISAXS is sensitive to both the surface morphology and the internal structure of thin films and is used to monitor the developing surface roughness.<sup>7</sup> The depositions and measurements were performed in the UHV film growth facility, adapted for thermal ALD, installed at beamline X21 of the National Synchrotron Light Source at Brookhaven National Laboratory.

The initial growth of HfO<sub>2</sub> on two Si based substrates (H-terminated Si and RCA cleaned Si) and two Ge based

substrates [H-terminated Ge and plasma-enhanced chemical-vapor deposition (PECVD) grown GeO<sub>2</sub>] was investigated. Tetrakis(ethylmethylamino)hafnium (TEMAH) and deionized water were used as Hf and O source, respectively. For Si-based devices, the main focus has been on HfCl<sub>4</sub> as Hf source, but promising results have been reported on the use of TEMAH for the growth of HfO<sub>2</sub> on Ge.<sup>8-12</sup> Because of the low vapor pressure of the TEMAH precursor, Ar was used as carrier gas. All experiments were carried out at a substrate temperature of 200 °C. An ALD cycle consisted of 8 s TEMAH (and Ar) exposure at 1.5 · 10<sup>-3</sup> mbar, 20 s pumping, 8 s water exposure at 10<sup>-3</sup> mbar, and again 20 s pumping. The lengths of the precursor steps were chosen so to ensure saturation.

The use of synchrotron-based x-rays allows for tuning of the x-ray energy. The incident x-ray energy was chosen to minimize the fluorescence from the substrate and maximize the fluorescence from Hf excitation. For all Si and Ge based experiments 10.8 and 10 keV x-rays were used, respectively. For the *in situ* XRF measurements, an incident angle of 5.25° was used and a silicon drift detector was positioned perpendicular to the sample, behind a Be window. XRF data were collected during the last pumping step of each ALD cycle. A XRF measurement took 20 s [Fig. 1(a)]. For the *in situ* GISAXS measurements, an incident angle near the angle of

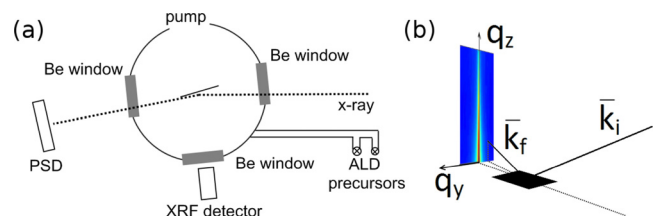


FIG. 1. (Color online) (a) Schematic top view representation of the UHV setup, adapted for ALD. X-rays hit the sample at a variable incidence angle. Scattered x-rays are observed with a PSD and fluorescent x-rays are observed by a silicon drift detector. (b) Schematics of the GISAXS geometry. Incident x-rays have a wave vector  $\mathbf{k}_i$ . Due to scattering the wave vector changes to  $\mathbf{k}_f$ . The momentum transfer due to scattering is denoted as  $\mathbf{q}$ .

<sup>a)</sup>Electronic mail: kilian.devloocasier@ugent.be.

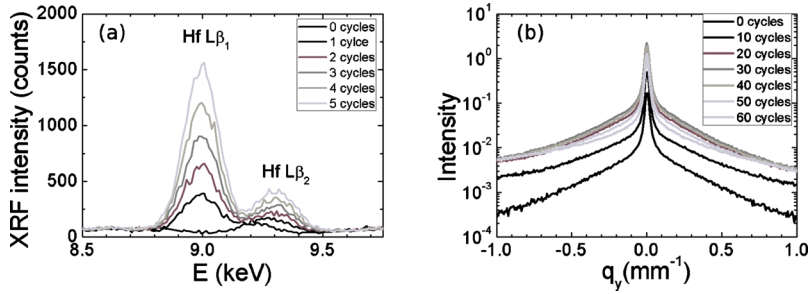


FIG. 2. (Color online) (a) Evolution of the Hf  $L_{\beta 1}$  (9.0 keV) and Hf  $L_{\beta 2}$  (9.3 keV) intensity as measured during the first ALD cycles on RCA cleaned Si. The Hf XRF intensity is proportional to the number of Hf atoms deposited. (b) Evolution of the GISAXS signal as measured every 10 ALD cycles on RCA cleaned Si.

total external reflection of the substrate was used and a one-dimensional position sensitive detector (PSD) was mounted at an exit angle of  $1^\circ$ , perpendicular to the plane of incidence. GISAXS measurements were performed every 10 cycles. The GISAXS data were collected by integrating the detector signal during a 60 s interval [Figs. 1 and 2(b)].

The results of the XRF measurements are displayed in Fig. 3. In this figure the integrated intensity of the Hf  $L_{\beta 1}$  emission line is plotted, as measured every ALD cycle [Fig. 2(a)]. Because the penetration depth of the incident x-rays is of the order of 500 nm, i.e., much larger than the thicknesses of the grown films, the XRF intensity can be used as a direct measure of the amount of deposited Hf atoms. This in turn enables the straightforward determination of the amount of  $\text{HfO}_2$  deposited during every single ALD cycle.

Note that *in situ* spectroscopic ellipsometry (SE) is often used for monitoring film growth during ALD.<sup>13</sup> The main advantage of the *in situ* XRF technique over the SE method is, especially during the very first ALD cycles, that XRF is not based on model fitting but allows for a direct characterization of the deposited (sub)monolayers, increasing the reliability of the results.

During the very first ALD cycles, hardly any growth retardation and a near-perfect linear growth is observed in the case of RCA cleaned Si and PECVD grown  $\text{GeO}_2$  [Figs. 3(b) and 3(d)]. This can be explained by the fact that the starting surfaces are at least partially OH-terminated. The hydroxyl groups have no trouble reacting with the TEMAH precursor, resulting in immediate growth without nucleation effects. Through post-deposition x-ray reflectivity measurements the final thickness could be determined, yielding a

growth per cycle (GPC) of  $1.2 \text{ \AA}$  per cycle on the Si substrate and  $1.6 \text{ \AA}$  per cycle on the Ge substrate. It is expected that the absence of a nucleation step results in relatively smooth layers, due to nice layer-by-layer growth. This was confirmed by ex situ atomic force microscopy (AFM) measurements (see Table I).

The growth of  $\text{HfO}_2$  on the H-terminated Si and Ge does not follow these characteristics. The XRF measurements clearly show that the amount of  $\text{HfO}_2$  deposited on the H-terminated Si and H-terminated Ge only starts increasing after 10 ALD cycles and 15 ALD cycles, respectively. This behavior corresponds to substrate-inhibited island growth as described by the model developed by Puurunen and Vandervorst.<sup>14</sup> In this model, one assumes that ALD growth only starts at certain defects. These defects then form small islands, which after sufficient amount of ALD cycles coalesce and form a continuous layer. From the XRF measurement, we also learn that the GPC on the H-terminated surfaces is much larger compared to the GPC on the oxidized surfaces. This can be explained by an increased roughness of the surface due to the island growth. A rough surface has a large surface area, leading to a higher GPC. The roughness of the  $\text{HfO}_2$  films after 100 ALD cycles and 70 ALD cycles on H-Si and H-Ge, respectively, was measured with ex situ AFM (see Table I). The AFM results are in agreement with previous ex situ studies of the nucleation of the TEMAH/ $\text{H}_2\text{O}$  process on Si based substrates under similar conditions.<sup>15</sup>

The evolution of the surface roughness during growth was studied by *in situ* GISAXS [see Fig. 2(b)]. In the low  $q_z$  limit, the integral of the GISAXS intensity can be used as a

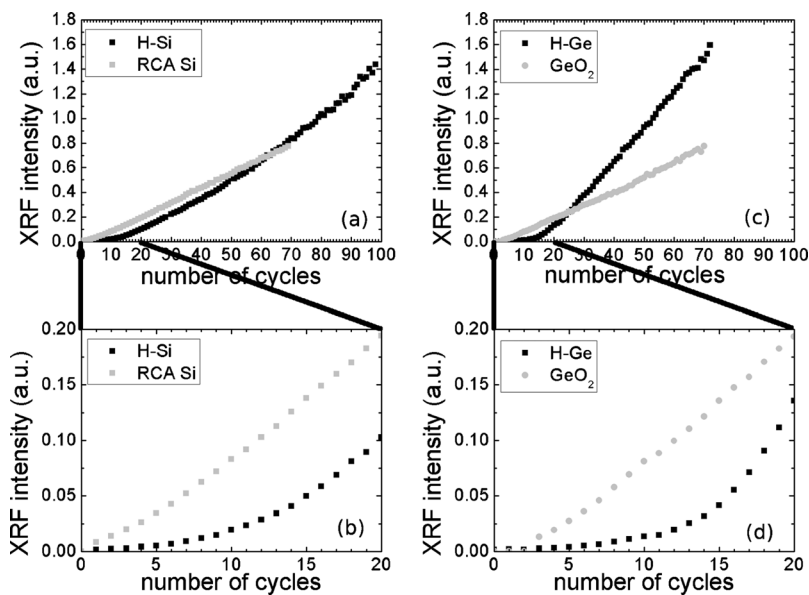


FIG. 3. Integrated Hf  $L_{\beta 1}$  fluorescence intensity measured during ALD on H-terminated Si and RCA cleaned Si [(a) and (b)] and on H-terminated Ge and  $\text{GeO}_2$  [(c) and (d)]. (b) and (d) are a detail of (a) and (c), respectively, focusing on the first 20 cycles.

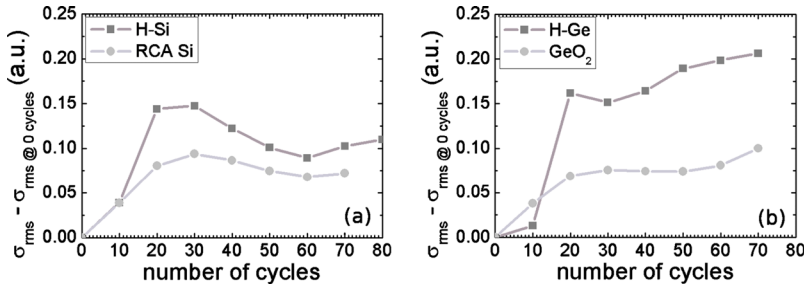


FIG. 4. (Color online) Roughness evolution based on the integrated GISAXS pattern for ALD on (a) H-terminated Si and RCA cleaned Si and on (b) H-terminated Ge and GeO<sub>2</sub>.

measure for the square of the rms roughness.<sup>7</sup>

$$\sigma_{\text{rms}}^2 \propto \int q_{\parallel} I(q_{\parallel}) dq_{\parallel}. \quad (1)$$

This enables a qualitative view on the roughness evolution during ALD deposition. The square root of this integral is displayed in Fig. 4 for the four samples at a 10 cycle interval. In order to focus on the increase in roughness, the initial integral at 0 cycles is subtracted from every value.

From this data several conclusions can be made. One immediately notices the higher roughness for the HfO<sub>2</sub> films grown on the H-terminated substrates compared to the oxidized substrates, confirming the AFM data. Furthermore, one observes that the film roughness only increases significantly during the initial growth phase. This again stresses the importance of the first ALD cycles. For the H-terminated substrates, one may also note that the roughness only starts increasing after about 10 to 20 cycles, confirming the idea that during the nucleation period, as seen with XRF, no significant amount of material is deposited. The similarities observed in the growth on the RCA cleaned Si and PECVD grown GeO<sub>2</sub> surfaces translates to a similar roughness evolution. Furthermore, for the Si substrates, the integral seems to have a minimum around 50 ALD cycles. This effect is caused by a variation in the peak height at  $q_{\parallel}=0$ . Because this peak has a nonzero width, the variation effect isn't totally eliminated by the weighing by  $q_{\parallel}$  in the integral. For the Ge substrates, this effect is less pronounced.

In conclusion, we have studied the initial ALD growth of HfO<sub>2</sub> on both oxidized and H-terminated Si and Ge surfaces by *in situ* XRF and GISAXS. These techniques enabled detailed characterization of the evolution of the amount of deposited material and surface roughness during growth. The ALD of HfO<sub>2</sub> on the oxidized surfaces showed no inhibition period and a layer-by-layer type growth. The HfO<sub>2</sub> growth

on H-terminated Si and Ge showed an inhibition period of 10 and 15 ALD-cycles, respectively. *In situ* GISAXS indicated a larger surface roughness for the HfO<sub>2</sub> films deposited on the H-terminated surfaces compared to the oxidized surfaces.

The research leading to these results has received funding from the European Research Council under the European Union's Seventh Framework Programme (Grant No. FP7/2007-2013)/ERC under Grant No. 239865. J.D. acknowledges the FWO-Vlaanderen for a scholarship. The Boston University component of this research was supported by the U.S. DOE Office of Science, Office of Basic Energy Sciences DE-FG02-03ER46037. Use of the National Synchrotron Light Source, Brookhaven National Laboratory, was supported by the U.S. Department of Energy, Office of Science, Office of Basic Energy Sciences, under Contract No. DE-AC02-98CH10886.

TABLE I. Root-mean-square roughness resulting from post-deposition AFM-measurements.

Substrate	H-Si	RCA Si	H-Ge	GeO <sub>2</sub>
$\sigma_{\text{rms}}$ (nm)	<b>0.717</b>	0.337	<b>1.020</b>	0.398

<sup>1</sup>S. M. George, *Chem. Rev.* **110**, 111 (2010).

<sup>2</sup>R. Puurunen, *J. Appl. Phys.* **97**, 121301 (2005).

<sup>3</sup>J. Robertson, *Eur. Phys. J.: Appl. Phys.* **28**, 265 (2004).

<sup>4</sup>J. Dendooven, S. P. Sree, K. D. Keyser, D. Deduytsche, J. A. Martens, K. F. Ludwig, and C. Detavernier, *J. Phys. Chem. C* **115**, 6605 (2011).

<sup>5</sup>J. Dendooven, D. Deduytsche, S. P. Sree, T. I. Korányi, G. Vanbutsele, J. A. Martens, K. F. Ludwig, and C. Detavernier, Proceedings of the AVS Topical Conference on ALD, Seoul, South Korea, 2010.

<sup>6</sup>D. D. Fong, J. A. Eastman, S. K. Kim, T. Fister, M. J. Highland, P. M. Baldo, and P. H. Fuoss, *Appl. Phys. Lett.* **97**, 191904 (2010).

<sup>7</sup>G. Ozaydin, K. F. Ludwig, H. Zhou, L. Zhou, and R. L. Haedrick, *J. Appl. Phys.* **103**, 033512 (2008).

<sup>8</sup>Q. Xie, J. Musschoot, M. Schaeckers, M. Caymax, A. Delabie, X.-P. Qu, Y.-L. Jiang, S. V. den Berghe, J. Liu, and C. Detavernier, *Appl. Phys. Lett.* **97**, 222902 (2010).

<sup>9</sup>Q. Xie, D. Deduytsche, M. Schaeckers, M. Caymax, A. Delabie, X.-P. Qu, and C. Detavernier, *Appl. Phys. Lett.* **97**, 112905 (2010).

<sup>10</sup>Q. Xie, D. Deduytsche, M. Schaeckers, M. Caymax, A. Delabie, X.-P. Qu, and C. Detavernier, *Electrochem. Solid-State Lett.* **14**, G20 (2011).

<sup>11</sup>Q. Xie, J. Musschoot, M. Schaeckers, M. Caymax, A. Delabie, D. Lin, X.-P. Qu, Y.-L. Jiang, S. V. den Berghe, and C. Detavernier, *Electrochem. Solid-State Lett.* **14**, G27 (2011).

<sup>12</sup>D. McNeill, S. Bhattacharya, H. Wadsworth, F. Ruddell, S. Mitchell, B. Armstrong, and H. Gamble, *J. Mater. Sci.* **19**, 119 (2008).

<sup>13</sup>E. Langereis, S. Heil, H. Knoops, W. Keuning, M. van de Sanden, and W. Kessels, *J. Phys. D* **42**, 073001 (2009).

<sup>14</sup>R. Puurunen and W. Vandervorst, *J. Appl. Phys.* **96**, 7686 (2004).

<sup>15</sup>J. Hackley and T. G. J. Demaree, *J. Appl. Phys.* **102**, 034101 (2007).